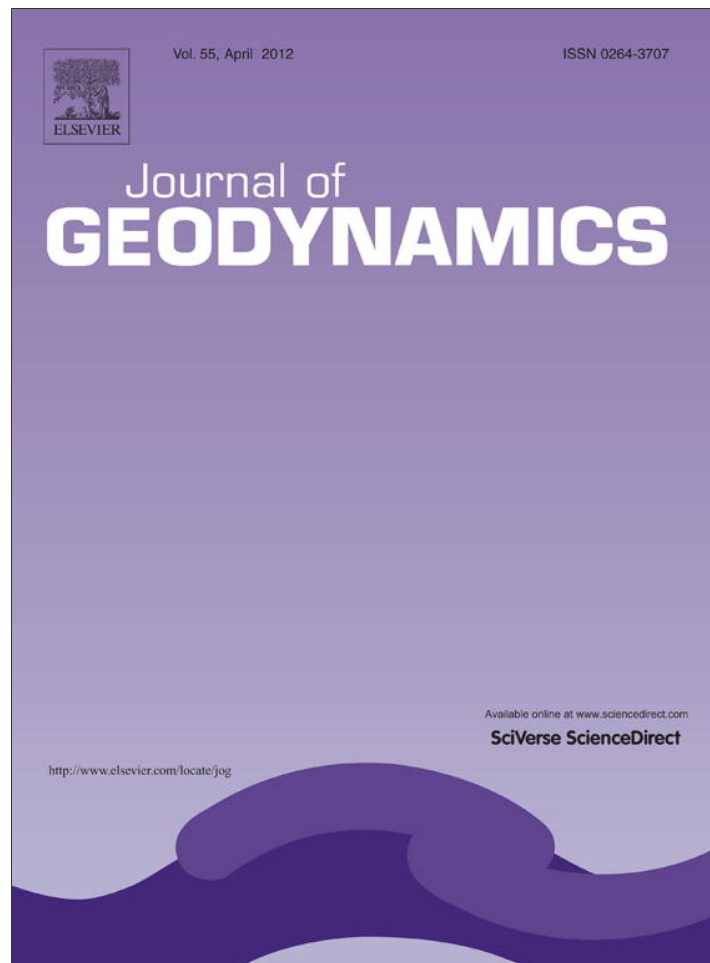


Provided for non-commercial research and education use.
Not for reproduction, distribution or commercial use.



This article appeared in a journal published by Elsevier. The attached copy is furnished to the author for internal non-commercial research and education use, including for instruction at the authors institution and sharing with colleagues.

Other uses, including reproduction and distribution, or selling or licensing copies, or posting to personal, institutional or third party websites are prohibited.

In most cases authors are permitted to post their version of the article (e.g. in Word or Tex form) to their personal website or institutional repository. Authors requiring further information regarding Elsevier's archiving and manuscript policies are encouraged to visit:

<http://www.elsevier.com/copyright>



Contents lists available at ScienceDirect

Journal of Geodynamics

journal homepage: <http://www.elsevier.com/locate/jog>

The role of elastic stored energy in controlling the long term rheological behaviour of the lithosphere

Klaus Regenauer-Lieb^{a,b,*}, Roberto F. Weinberg^c, Gideon Rosenbaum^d

^a School of Earth and Geographical Sciences, The University of Western Australia, Perth, Western Australia 6009, Australia

^b CSIRO Earth Science and Resource Engineering, Kensington, Western Australia 6151, Australia

^c School of Geosciences, Monash University, Clayton, Victoria 3800, Australia

^d School of Earth Sciences, The University of Queensland, Brisbane, Queensland 4072, Australia

ARTICLE INFO

Article history:

Received 8 June 2011

Received in revised form 8 August 2011

Accepted 8 August 2011

Available online 7 September 2011

Keywords:

Lithosphere

Rheology

Numerical modelling

Continental strength

ABSTRACT

The traditional definition of lithospheric strength is derived from the differential stresses required to form brittle and ductile structures at a constant strain rate. This definition is based on dissipative brittle and ductile deformation and does not take into account the ability of the lithosphere to store elastic strain. Here we show the important role of elasticity in controlling the long-term behaviour of the lithosphere. This is particularly evident when describing deformation in a thermodynamic framework, which differentiates between stored (Helmholtz free energy) and dissipative (entropy) energy potentials. In our model calculations we stretch a continental lithosphere with a wide range of crustal thickness (30–60 km) and heat flow (50–80 mW/m²) at a constant velocity. We show that the Helmholtz free energy, which in our simple calculation describes the energy stored elastically, converges for all models within a 25% range, while the dissipated energy varies over an order of magnitude. This variation stems from complex patterns in the local strain distributions of the different models, which together operate to minimize the Helmholtz free energy. This energy minimization is a fundamental material behaviour of the lithosphere, which in our simple case is defined by its elastic properties. We conclude from this result that elasticity (more generally Helmholtz free energy) is an important regulator of the long-term geological strength of the lithosphere.

Crown Copyright © 2011 Published by Elsevier Ltd. All rights reserved.

1. Introduction

Lithospheric strength profiles typically include a brittle upper crust overlying a viscous lower crust and a mantle that can behave as a ductile layer or change from brittle to ductile behaviour with depth (Goetze and Evans, 1979; Kohlstedt et al., 1995). The resulting curve, known as the Brace–Goetze strength profile (or ‘Christmas Tree’), provides a general and simple framework for understanding lithospheric behaviour and is commonly used to solve geodynamic problems (e.g. Burov et al., 1998; Molnar, 1992; Moresi and Solomatov, 1998; Schmalholz et al., 2009). In this framework, the strength of the lithosphere is defined as the differential stress that it sustains when deforming at a constant strain rate integrated across a one dimensional section (Ranalli and Murphy, 1987).

The Brace–Goetze strength profile and much of our current view of lithospheric strength is based on its dissipative structures, such as brittle and viscous deformation. This is essentially a fluid

dynamic definition of strength. The current debate on lithospheric strength is focussed on two end-member dissipative models, the so-called ‘jelly sandwich’ and ‘crème brûlée’ models. The lithosphere considered in the ‘jelly sandwich’ model is characterized by a weak lower crust in between a strong upper crust and upper mantle (Afonso and Ranalli, 2004; Burov, 2010; Burov and Watts, 2006). According to the second model, in contrast, the lithospheric strength resides entirely in the upper crust (Jackson, 2002), thus explaining the scarcity of seismicity in the upper mantle (Maggi et al., 2000).

In the context of this debate, little attention has been given to the role of elasticity and the solid mechanical behaviour of the lithosphere. Elasticity is known to play a major role, particularly during stress loading of the lithosphere, through its power to amplify stresses in the strongest sections of the rock pile (Kusznir, 1982). In this paper, we combine the views from fluid dynamics and solid mechanics to investigate the integrated rheological response of the lithosphere to deformation. Using elasto-viscoplastic numerical models of lithospheric extension, we investigate the evolution of the dissipated energy and the stored elastic energy of the whole system. Our models incorporate time explicitly into the solution of slow deformation, thereby providing strength

* Corresponding author at: The University of Western Australia, School of Earth and Geographical Sciences, 35, Stirling Ave, Perth, Western Australia 6009, Australia.
E-mail address: reg025@csiro.au (K. Regenauer-Lieb).

evolution derived from energy fluxes. Within this thermodynamic framework, we apply a global homogenisation method and obtain an upper bound for the strength of the lithosphere in an integral form. Our results show that for given elastic properties, the value of the integrated strength remains relatively constant regardless of changes in crustal thickness and surface heat flow. Conversely, we postulate that it is the ability of the lithosphere to store elastic strain energy that plays a crucial role in determining the long-term rheological behaviour of the lithosphere.

2. Definition of elastic strength of the lithosphere

The classical Brace–Goetze definition of strength simplifies the behaviour of the lithosphere by considering a 1D section deforming at constant strain rate and excluding any complexities related to elastic stress amplification (e.g. Kuszniir, 1982; Kuszniir and Park, 1982, 1984). This definition is only based on dissipation mechanisms and does not consider time evolution aspects and feedbacks between stored and dissipated energies. In an elasto-visco-plastic rheology, energy can be stored at any given point of the deformational history, and may significantly affect the strength of the lithosphere through the formation of interlinked localized shear zones. Therefore, from a thermodynamic perspective it is important to consider how the energy is stored, dissipated and transferred across the volume as the system equilibrates. The fundamental question is how the stored and dissipated energy are linked in a larger scale in controlling the global integrated strength and how we can incorporate this element in the definition of lithospheric strength.

Deformation of the lithosphere is commonly illustrated in stress versus strain diagrams (Fig. 1). During shear loading there is initially a period of elastic deformation, where stress increases linearly and energy is stored in the form of recoverable, elastic strain. The slope of this linear section of the curve is controlled by the average elastic shear modulus of the lithosphere. When stresses reach the yield point, inelastic deformation of the lithosphere takes over, and energy is then dissipated as rocks yield. Two different models are used in geodynamics to define the strength of the lithosphere. Commonly, a fluid dynamics visco-plastic definition of strength is used, whereby the strength is derived from viscosity profiles disregarding the elastic properties of the lithosphere. This approach emphasizes the role of strain rate dependence (Fig. 1a), which varies as a function of Moho temperature, viscosity profile of the lithosphere and plastic yield strength. In contrast, in solid mechanics elasto-plastic approaches, the yield strength is the elastic limit.

We merge the solid-mechanics and fluid dynamics definitions of strength and define an “elastic strength”, calculated from the

stored elastic energy (shaded triangular areas under the curves in Fig. 1). This definition takes into account all components of an elasto-visco-plastic rheology: the elastic moduli of the rock mass, its yield strength and its instantaneous viscosity. It can be understood as an elastic stiffness measure, allowing the lithosphere to be strong either due to high yield strength/flow stress (Fig. 1a) or low elastic moduli (Fig. 1b). This implies that under the same kinematic boundary conditions, a lithosphere with a low elastic modulus can sustain a higher strain before reaching the elastic limit than a lithosphere with a high elastic modulus.

3. Numerical modelling: elastic versus dissipative strength

3.1. Modelling approach

Our modelling approach considers feedback effects between brittle and ductile localization phenomena. Such feedback effects lead to strain localization and allow for weakening of the integrated strength of the lithosphere, as described in previous publications (Braeck and Podladchikov, 2007; Kaus and Podladchikov, 2006; Regenauer-Lieb et al., 2008, 2006; Regenauer-Lieb and Yuen, 2003; Rosenbaum et al., 2010). In this paper, the emphasis is the modelling of the integrated global evolution of the elastic and dissipative strengths, for which we use five coupled balance equations: the continuity equation the conservation laws of linear and angular momentum, the energy balance and the entropy exchange. The science dealing with the last equation is known as non-equilibrium thermodynamics (Prigogine, 1978). By solving all five equations, we are able to couple the stored energy with the dissipated energy. The discussion below focuses on the thermodynamic methodology. Further details on the thermodynamic approach for modelling shear zones are outlined in Regenauer-Lieb and Yuen (2003). More recent contributions on the applied method for analyzing seismic and geodynamic instabilities (Regenauer-Lieb et al., 2009), geo-materials damage (Karrech et al., 2011a,c) and frame indifference (Karrech et al., 2011b), as well as the incorporation of chemistry (Poulet et al., 2010) are also available. A complete description of the first four equations is outlined in Rosenbaum et al. (2010).

The internal energy U of any body can be decomposed into two energy components, which are the Helmholtz free energy $\psi(T, \varepsilon_{ij}^{el}\{\alpha_k\})$ and the entropy S , respectively:

$$U = \psi(T, \varepsilon_{ij}^{el}\{\alpha_k\}) + ST \quad (1)$$

The Helmholtz free energy describes the stored energy characterized by the set of independent variables $T, \varepsilon_{ij}^{el}, \{\alpha_k\}$, where T is the absolute temperature, ε_{ij}^{el} is the elastic part of the local

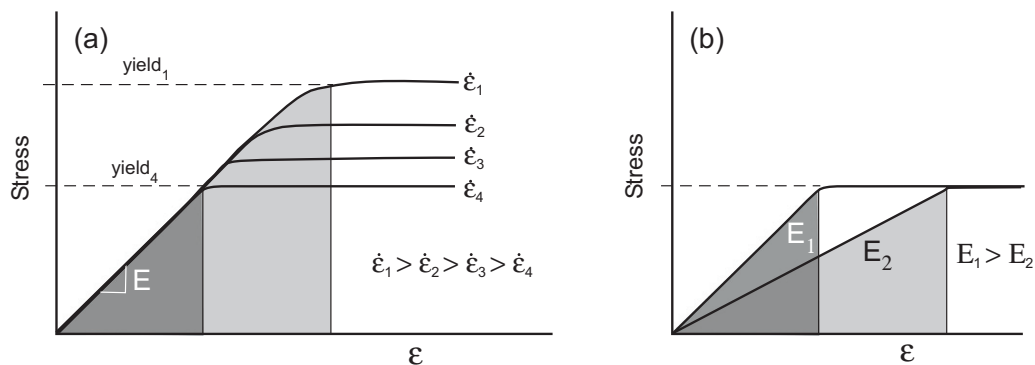


Fig. 1. Stress versus strain plot showing curves for different lithospheres. The classic definition of lithospheric strength is the yield strength as a function of strain rate, temperature, flow laws and plastic yield. The initial linear slope of the curves is controlled by the Young's modulus (E) and all curves in (a) have the same modulus (b) Young's modulus changes and elastic strength is defined here as yield strength times half the strain (triangular regions in grey). This definition gives rise to two possible types of strong lithosphere (large triangles): one with high yield strength (tall triangle in (a)), the other with low Young's modulus (triangle in (b)).

total strain tensor $\varepsilon_{ij} = \varepsilon_{ij}^{el} + \varepsilon_{ij}^{diss}$, and $\{\alpha_k\}_{k \leq n}$ are a set of n local internal state variables considered in a Lagrangian material framework. Energy in our calculation is only stored in elastic deformation (shear and volume changes) controlled by the elastic shear and bulk modulus. In nature, there are other ways to store energy, meaning that $\{\alpha_k\}_{k \leq n}$ variables can describe chemical strains, electrical charges, damage or any other microstructural parameters, such as dislocation density or grain size. Here we only consider thermal expansion α_{th} as the third independent variable in the Helmholtz free energy. The entropy is defined through the second law of thermodynamics

$$dS \geq \frac{\delta Q}{T} \quad (2)$$

where d represents an infinitesimal small change of a state function, δ represents an infinitesimal small change of a path function and Q is the heat. In a given material volume, the entropy can be decomposed further into a component of heat that flows in and out of the volume at its boundaries, and a component of entropy production inside the volume itself:

$$dS = \delta S_{surf} + \delta S_{diss} \quad (3)$$

where d indicates a complete differential and δ an incomplete, i.e. path-dependent, differential.

Without loss of generality, we consider in this paper only heat flow through conduction $\rho c_p \kappa \nabla^2 T$ at the boundaries of Lagrangian finite volume elements where ρ is the density, c_p is the specific heat and κ the thermal diffusivity. For the dissipation inside the elements, we only consider shear heating and internal radiogenic heat production r_i . In this paper we assume that the conversion of mechanical work into heat by the dissipative strain rates $\dot{\varepsilon}_{ij}^{diss}$ occurs at 100% conversion efficiency. This conversion efficiency is close to the experimental value (Chrysochoos and Belmahjoub, 1992) and also follows from our choice of the state variable in the Helmholtz free energy, i.e. we assume that no deformational work is stored in microstructural defects. In this case, shear heating is simply the product of the Cauchy stress tensor σ_{ij} times the dissipative strain rate $\dot{\varepsilon}_{ij}^{diss}$ describing plastic or viscous deformation.

Although the entropy approach is a very powerful method for describing time-dependent upper and lower bounds of energy flows during the mechanical evolution of deforming solids (Regenauer-Lieb et al., 2010), we see from Eq. (3) that it is slightly more complex than the comparatively simple Helmholtz free energy approach. Therefore, we choose in this paper to describe elastic strength by the Helmholtz free energy potential and not its conjugate potential, the irreversible entropy production also known as internal dissipation. In varying only thermodynamic flux boundary conditions (velocity and heat flow) rather than thermodynamic force boundary conditions (applied stress and temperature), we obtain an estimate of an upper bound of dissipation (Regenauer-Lieb et al., 2010).

The rate of Helmholtz free energy production can be decomposed using the chain rule:

$$\dot{\psi}_{T, \varepsilon_{ij}^{el}, \{\alpha_k\}} = \left(\frac{\partial \psi}{\partial T} \right)_{\varepsilon_{ij}^{el}, \{\alpha_k\}} \dot{T} + \left(\frac{\partial \psi}{\partial \varepsilon_{ij}^{el}} \right)_{T, \{\alpha_k\}} \dot{\varepsilon}_{ij}^{el} + \left(\frac{\partial \psi}{\partial \alpha_k} \right)_{T, \varepsilon_{ij}} \dot{\alpha}_k \quad (4)$$

Using this approach and considering the entropy production (Eq. (3)), we can derive the classical energy equation (Regenauer-Lieb et al., 2009) by differentiating the first law with respect to time and considering the constraint from the second law which leads to:

$$\int_V \rho c_p \frac{DT}{Dt} dV = \int_V \sigma_{ij} \dot{\varepsilon}_{ij}^{diss} dV - \int_V \rho \frac{\partial \psi}{\partial \alpha_j} \frac{D\alpha_j}{Dt} dV + \int_V \rho T \frac{\partial^2 \psi}{\partial T \partial \alpha_j} \frac{D\alpha_j}{Dt} dV + \int_V r_i dV - \int_A r_a dA - \int_A q_a dA \quad (5)$$

Where the first two terms on the right side of the equation describe shear heating (Eq. (6)), the third term is the thermomechanical coupling term, the fourth term the internal heat generation through e.g. radioactive decay, Joule heating, chemical reactions etc., the fifth term describes the surface heat transfer by radiation and the sixth term the surface heat transfer by conduction.

We note, that additional feedback terms must be considered in the energy equation. One feedback stems from the dissipative strain. The dissipated energy feedback term is known as the shear heating term:

$$\int_V \dot{W}_{diss} dV = \int_V \sigma_{ij} \dot{\varepsilon}_{ij}^{diss} dV - \int_V \rho \frac{\partial \psi}{\partial \alpha_j} \frac{D\alpha_j}{Dt} dV \quad (6)$$

In this paper the time-dependent second term in Eq. (6) is neglected as noted earlier. New important feedback terms also appear as partial derivative of the Helmholtz free energy. We call these terms the thermal-mechanical coupling terms. The terms describe the effect of the state variable on the energy equation. If we consider for instance as state variable the elastic volumetric strain then we obtain an elastic energy feedback term which is sometimes known as thermo-elastic or isentropic work term and is:

$$\int_V \dot{W}_{isent} dV = \int_V \rho T \frac{\partial^2 \psi}{\partial \varepsilon^{el} \partial T} \dot{\varepsilon}^{el} dV \equiv \int_V \alpha_{th} T_{equ} \dot{p} dV \quad (7)$$

This isentropic work is here given in the conjugate Helmholtz and the Gibb's reference frames (change of the state variable strain for pressure), where α_{th} is the thermal expansion coefficient at the equilibrium temperature T_{equ} and \dot{p} is the time derivative of pressure. Another example would be to consider as a state variable the fractional volume of a particular phase which leads directly to the latent heat release term in the energy equation (see, Regenauer-Lieb et al., 2009).

These additional work terms in the energy equation correspond to thermal-mechanical couplings and are normally not considered in mechanical calculations.

Since the boundary conditions for our model have been chosen such that the radiogenic heat production and the heat conduction together are those corresponding to a steady state geotherm, these two terms are key energetic terms to the time-dependent evolution of the elastic strength.

The calculations use a far-from equilibrium thermodynamic approach. Time-dependent solutions are obtained by the coupled temperature-displacement solver in ABAQUS (ABAQUS/Standard, 2000), which adjusts time steps according to convergence criteria in both momentum and energy equations (see also Regenauer-Lieb et al., 2008, 2006; Regenauer-Lieb and Yuen, 2004). The initial undeformed box of 80 km deep and 100 km wide consists of 98 by 196 nodes.

3.2. Advantages and disadvantages of the thermodynamic approach

The thermodynamic approach is computationally more expensive than the classical mechanics approach. One may therefore want to mix elements of the thermodynamic approach with the classical mechanics approach. Unfortunately this mixture is not permissible from a thermodynamic point of view. If we use, for instance in one and the same model a layer that can deform by shear heating instability and add a layer with a Mohr-Coulomb behaviour

the entropy of the entire system is altered through the addition of this non-conservative layer. In a thermodynamic approach the Mohr–Coulomb layer must be replaced by a more complex formulation that is derived from the dissipation function and its Legendre transform (Karrech et al., 2011a,c). This ensures that all thermodynamic fluxes are handled consistently. The main limitation of the thermodynamic approach hence is that all localization mechanism have to be derived explicitly from the dissipation function and the feedback terms rather than postulated. A mixed approach is therefore better viewed as an extension to the classical mechanical approach rather than a thermodynamic approach.

The main difference between the thermodynamic and the classical mechanics approach is that the thermodynamic method is based on a time-dependent and not a quasistatic formulation. Another important difference is that the approach is based on a postulate of the Helmholtz free energy and a dissipation function, which are derived from the physics considered. The plasticity law and flow rules are then derived through the Legendre transform. This is fundamentally different to classical mechanics, where we start with a postulated elasticity law and a plasticity law as well as a flow rule. Time does not enter the equation. The classical mechanical approach therefore gives the investigator a larger degree of freedom to formulate plasticity laws and flow rules according to a known fit to experimental results. This is because classical mechanics is not constrained by the physics of the processes thus offering additional degrees of freedom and additional fitting parameters. Fitting parameters are limited in the thermodynamic method through the minimization of the dimensionality of the problem by the independent thermodynamic state variables. Classical mechanical solutions are also not constrained by the need to consider the explicit calculation of irreversible entropy production S_{dis} on top of the classical balance entropy fluxes S_{surf} .

In brief, both methods have their advantages and disadvantages, the physicist might prefer the computationally more demanding thermodynamic approach while the engineer might prefer the classical mechanics approach. In practice one may want to use both methods in series using thermodynamically inspired upscaling

methods. As a first step we recommend to investigate the geological problems with the full thermodynamics approach. This is because geological deformation is beyond the control of laboratory experiments and there are no data of material behaviour on millions of years time scale available. The thermodynamics approach allows the researcher to generate such data and constrain long-term material prediction from first principles. In a second step one may then again wish to revert to the classical approach and simplify the results of the thermodynamic approach in order to save computational resources.

A significant added value of the explicit entropy-based formulation is that time-dependent weakening and the width of the shear zone are all derived from the energy fluxes and the irreversible entropy production. This implies that for the ideal case, where the fundamental physics has been identified and the entropy formulation is used correctly, there is no mesh sensitivity, see also: (Regenauer-Lieb and Yuen, 2004) and (Karrech et al., 2011a). The distance between shear zones also relies on the energy fluxes and large strain can be achieved.

3.3. Model setup

The model setup considers lithospheric extension with varying crustal thicknesses and heat flows, while keeping material parameters constant. The rheology used is serial elasto-visco-plastic with a power-law viscous flow and a Goetze criterion for plastic yielding (see Table 1 for parameters). The effects of magmatism, which provide an alternative mechanism for continental break-up (Buck, 2006), were not considered. We use a simple horizontally stratified rheology of the top 80 km of the lithosphere, subject to a constant half-extension velocity of 0.6 cm/a applied to the left and right boundaries of the model. This is a typical rifting velocity prior to continental breakup comparable to estimates for the non-volcanic Galicia margin (half-extension velocity 0.4–1 cm/a) (Pérez-Gussinyé et al., 2006). Loading is gradual and occurs by accelerating the boundaries from zero to the final velocity over a period of ~100,000 years.

Table 1
Parameters used in the numerical model.

Parameter	Name	Value	Units
Temperature control			
χ	Shear heating efficiency	1	–
κ	Thermal diffusivity	Quartz = 0.7×10^{-6} Feldspar = 0.7×10^{-6} Olivine = 0.8×10^{-6}	$\text{m}^2 \text{s}^{-1}$
λ	Thermal expansion	3.1×10^{-5}	K^{-1}
c_p	Specific heat	1200	$\text{J}/(\text{kg K})$
ρ	Density	Quartz = 2800 Feldspar = 2800 Olivine = 3300	kg/m^3
B	Thickness of the radiogenic layer (top of crust)	10	km
Q_s	Surface heat flow	50–80	mW/m^2
Q_m	Mantle heat flow	20	mW/m^2
Elasticity			
ν	Poisson ratio	0.3	–
E	Young's modulus	4.5×10^{10} (all models except Fig. 5b where $E = 4.5 \times 10^9$ Pa)	Pa
Viscous flow law			
A	Material constant—pre-exponential parameter	Quartz = 3.98×10^{-21} Feldspar = 7.94×10^{-26} Olivine = 3.6×10^{-16}	$\text{Pa}^{-n} \text{s}^{-1}$
N	Power-law exponent	Quartz = 2.6 Feldspar = 3.1 Olivine = 3.5	–
H	Activation enthalpy	Quartz = 134 Feldspar = 163 Olivine = 480	kJ/mol
Plasticity			
	Yield shear stress (τ) = lithostatic pressure (P) (Goetze criterion)		

Values for A , H and n for wet quartzite and feldspar are from Kirby and Kronenberg (1987a,b), and for olivine from Hirth and Kohlstedt (2004).

The lithosphere below 80 km depth is considered to have a negligible contribution to the integrated strength. In the model, the lithosphere is extended horizontally from an initial 100 km width to 264 km at the end of the calculations over 13.7 million years. The top of the model is a free boundary while the bottom is horizontal and frictionless. This neglects processes in the deeper part of the lithosphere. The lithosphere has three rheological layers: the top layer (two thirds of the crust) is comprised of quartz-dominated rocks, the bottom third is comprised of feldspar-dominated rocks, and the mantle is comprised of olivine-dominated rocks. The heat flow at the bottom of the lithosphere is kept constant in the parametric study (20 mW/m^2) and the initial radiogenic heat contribution to the top 10 km of the crust is varied in the range of $30\text{--}60 \text{ mW/m}^2$ in 10 mW/m^2 increments, such that the flux at the top is equal to $50\text{--}80 \text{ mW/m}^2$ at steady state at the start of extension. We also varied the total crustal thickness from 30 to 60 km in increments of 10 km for each surface heat flow from 50 to 80 mW/m^2 .

4. Results

4.1. Temporal evolution of the stored and dissipative energies

The deformation resulting from stretching two models with different initial thermal profiles (i.e. different initial heat flows) are shown in Fig. 2. In the models, the local stored energy is the recoverable component of deformation, calculated for a given element as

the integral of the stress multiplied by the elastic strain rate over a time step. The global stored energy (e.g., Fig. 3a) is the local stored energy integrated over the entire model volume. The dissipative energy is the non-recoverable component, which is here assumed to be entirely transformed into heat, and given as the integral across the model and over one time step (Fig. 3b).

The strain distribution of the two models shows that the hotter lithosphere is characterized by diffuse deformation whereas the colder lithosphere has localized shear zones. The colder model (Fig. 2a) is characterized by high strain shear bands (grey: $>200\%$ strain) surrounding weakly strained blocks (darker blue tones $<50\%$ strain). In contrast, the hotter case (Fig. 2b) has lower strain shear bands (yellow to red: $180\text{--}150\%$ strain) and widespread straining of intervening blocks (green to light blue: $100\text{--}50\%$ strain). The strongly localized strain in Fig. 2a is reflected by its abrupt Moho topography, in contrast to the gentle Moho undulations in Fig. 2b indicative of generalized flow. This difference in pattern and degree of localization reflects differences in local stored energy and dissipated energy. Despite the obvious differences in dissipative structures, when local stored energy is integrated (Fig. 3a), the results are nearly identical. This indicates that, despite thermal and compositional differences, models have effectively the same elastic strength (i.e., ability to resist a given applied force). When comparing all sixteen models (Fig. 4), results show that despite significant difference in initial crustal thickness and heat flow, all modelled elastic strengths follow close paths, with values that do not differ more than 25% from each other at any point (Fig. 4a).

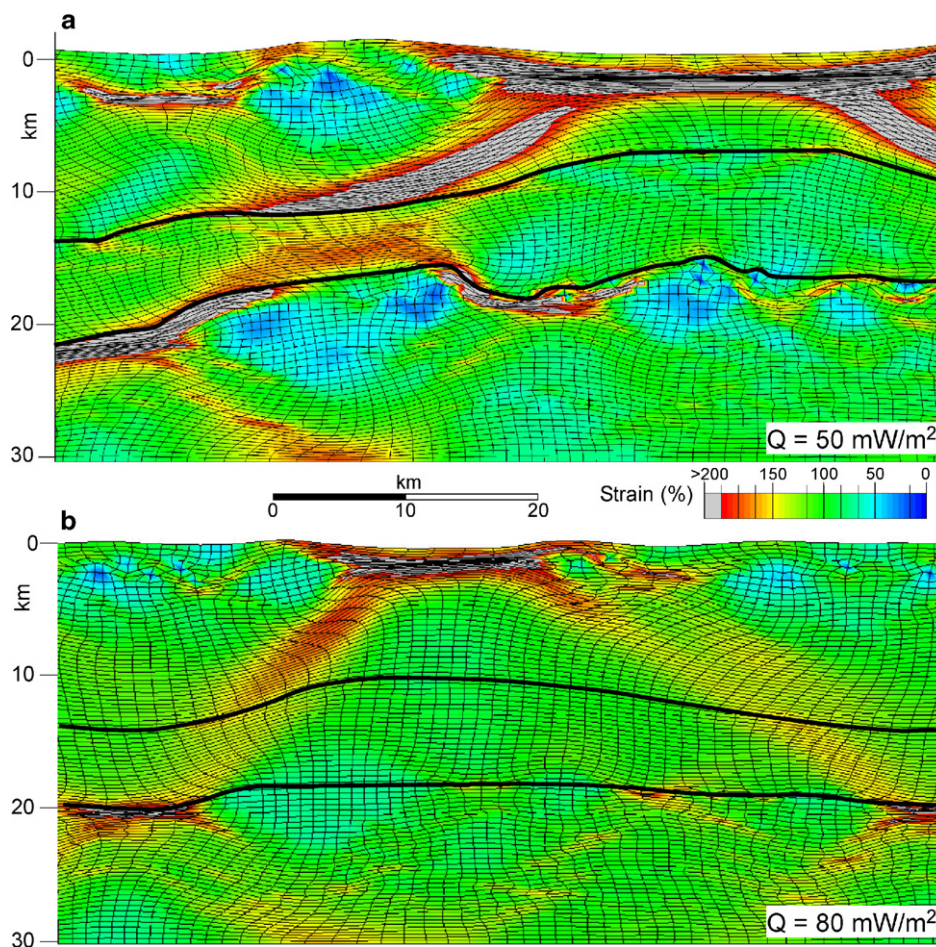


Fig. 2. Finite strain distribution after 13.7 Ma and $\beta = 2.6$ for models with initial crustal thickness of 50 km and heat flow of (a) 50 mW/m^2 , (b) 80 mW/m^2 . The two thin black lines define boundaries between quartz-, feldspar- and olivine-dominated layers, with the lower line corresponding to the base of the crust (Moho). For dissipation distribution in (a) see Fig. 7.

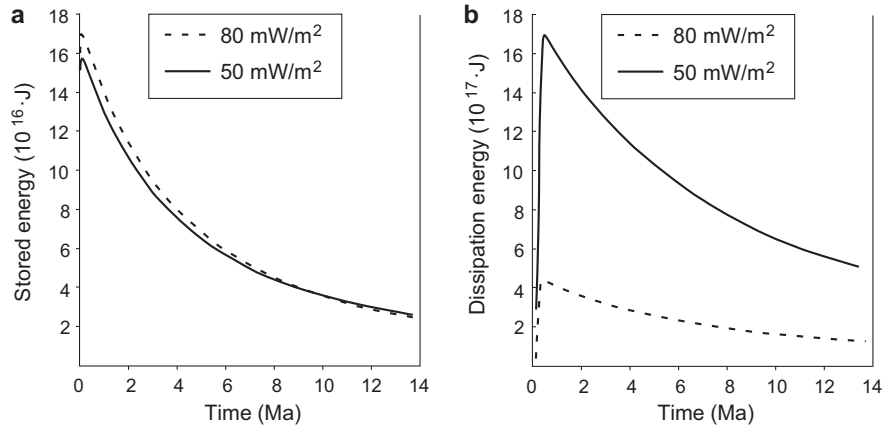


Fig. 3. (a) Evolution of the global elastic stored energy. Surprisingly, the stored energy curves are similar despite significant variations in the local stored energy causing the differences in the straining patterns (see Fig. 2). The time integrated strength difference between the two models is 17% and is due to the degree of strain localization. (b) Evolution of the dissipated energy per time step (10^{10} s). In contrast to the stored energy, the dissipated energy varies by a factor of four.

This behaviour contrast with, and is a response to, energy dissipation (Figs. 3a and 4b). The early stage of stress loading is characterized by relatively little energy dissipation, because most of the energy is being stored elastically. This stage is followed by an abrupt increase in energy dissipation, marking a period of transition from effective elastic behaviour of the model lithosphere to yielding. Dissipation of energy reaches a peak and then gradually decreases with time. In contrast to stored energy, dissipation energies vary by a factor of nine (Fig. 4b). The colder models dissipate more energy when compared to the hotter models, and in doing so, they achieve the same amount of stored energy. Similar calculations with applied boundary velocity decreased by one order of magnitude (Fig. 5a), maintaining the same shear modulus, show that the stored energy converged to the very same absolute values. In contrast, when shear modulus was decreased, the ability of the lithosphere to store energy was significantly increased (Fig. 5b). We find a profound influence of the elastic parameters on the elastic strength.

This result is one of the key findings of this paper highlighting the fundamental role of elasticity in controlling the strength of the lithosphere. It may have far reaching consequences for future modelling of lithospheric strength. One next logical step is to investigate the time-dependent evolution of elasticity in the context of a thermodynamic approach. This would allow us to investigate evolving lithosphere strength as a function of elastic property changes due

to weakening of elastic properties by e.g. brittle, ductile and creep failure. Recently, we have incorporated the full range of the mentioned failure mechanisms in a thermodynamic, damage mechanics formulation (Karrech et al., 2011a,c) and extended it to finite strain (Karrech et al., 2011b). The aspect of evolving elastic properties due to partial melting is still an ongoing research area.

Peak stress load in the models was reached after $\sim 10^{13}$ s, showing maximum energy values that do not exceed those likely to arise from plate tectonics. This implies that feedback effects weaken even the potentially strongest models, thus limiting the amount of energy required for deformation, regardless of the thermal and rheological structure of the modelled lithosphere (Fig. 4). We note, however, that these results would not necessarily apply outside the ranges of common plate tectonic velocities and rock type flow rheologies.

In detail, elastic strength curves cross each other, gently diverging or converging with time. In the initial deformation step, the elastic strength does not define clear variations with initial input parameters (Fig. 6a). In contrast, at a mature stage, a pattern of elastic strength variation emerges (Fig. 6b), associated with weaker models for initially thicker crust, as expected, but also weaker models for cooler lithospheres. The small variations in time-dependent elastic strengths for all models, despite significant variations in crustal thicknesses and heat flows, are in sharp contrast to classical modelling solutions where two to three orders of magnitude

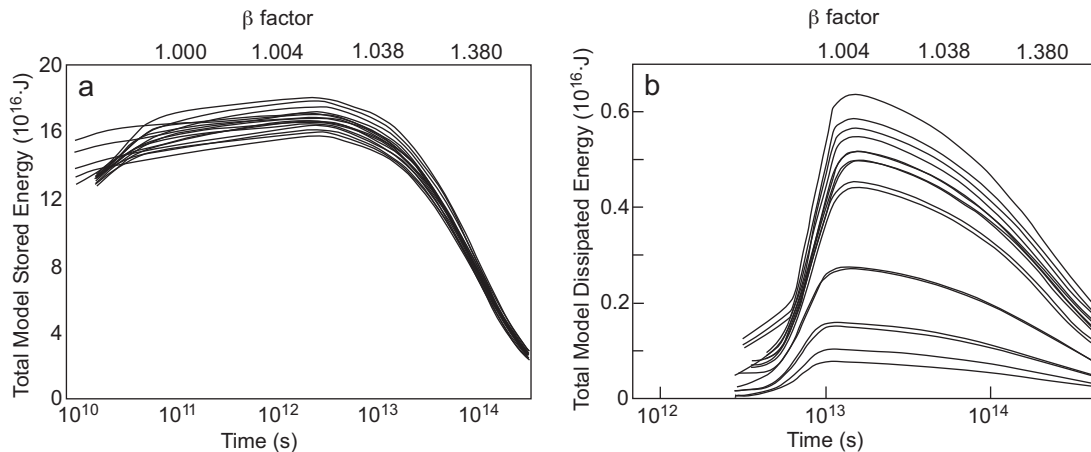


Fig. 4. Time evolution of the stored (elastic) energy (a) and dissipated energy (b) for all models, with initial and final values plotted in Fig. 6 (note logarithmic time x-axis). All models in (a) follow similar paths (see text). The initial positive slope reflects a linear increase in velocity from 0 to 1.2 cm/a during the first 10^{13} s, equivalent to $\beta = 1.04$.

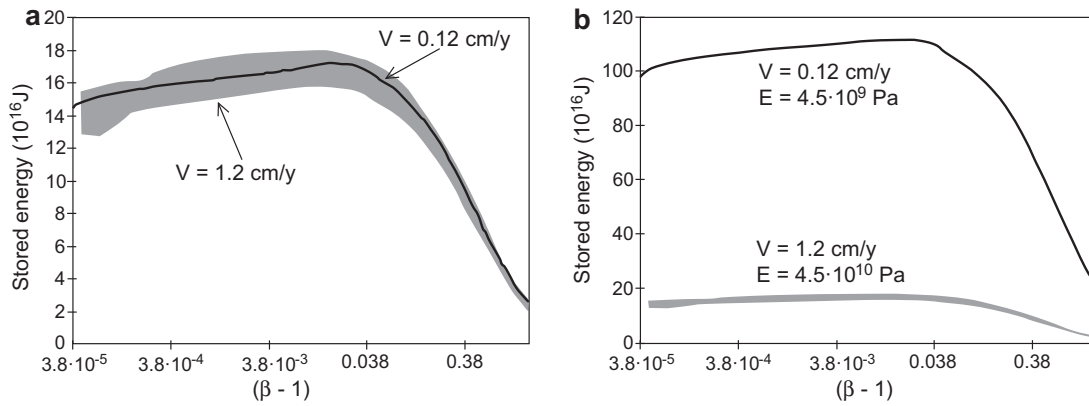


Fig. 5. Similar runs to those plotted in Fig. 4 with initial crustal thickness of 50 km and heat flow of 60 mW/m². (a) Results with an imposed boundary velocity one order of magnitude lower, coinciding with the field defined by all 16 models in Fig. 4a (grey area). (b) Results with both boundary velocity and Young's modulus reduced by one order of magnitude (black line). Comparison with results from Fig. 4a (narrow grey band at the bottom of the diagram) indicates that reduction of Young's modulus leads to a factor of seven increase in stored energy. Diagrams show that the evolution of the elastic strength is insensitive to changes in the boundary velocity (a), but is strongly modified in response to changes in the elastic properties (b).

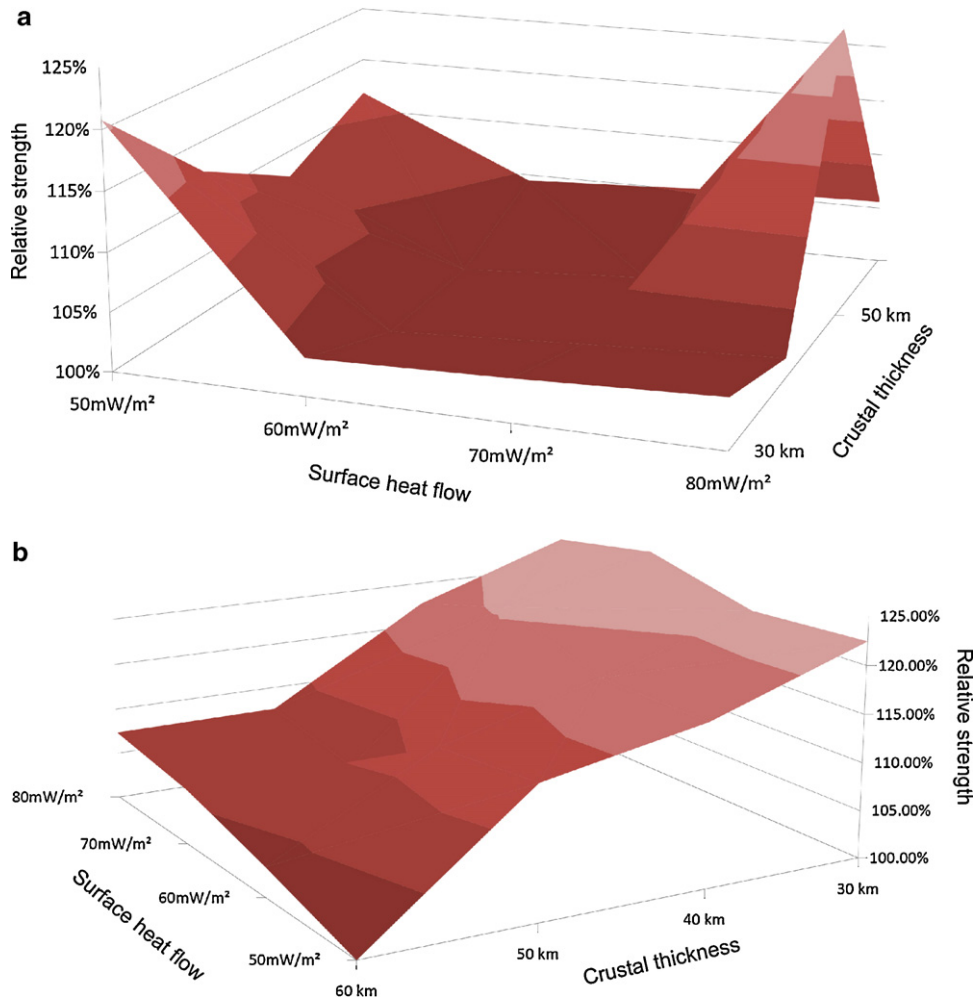


Fig. 6. Summary diagram illustrating how changes in the surface heat flow and crustal thickness affect the elastic strength. The diagram shows the strength (see Fig. 4a) at the initial time step (a) and the final step (b). In order to highlight differences in the elastic strength, all models are divided by the lowest strength value (for the corresponding time step). This normalized strength is called here the relative elastic strength. Note that the relative elastic strength varies for both time steps (a) and (b) by less than 27%. The plot reveals that the elastic strength is lowest at the initial time step (a) for models with intermediate heat flow (60 and 70 mW/m²) while there does not appear to be a correlation with crustal thickness. For the final step (b), the model reveals a significant trend of decreasing elastic strength with increasing crustal thickness while there appears to be a weak trend of decreasing elastic strength with decreasing surface heat flow.

of strength variation are expected (Perry et al., 2006). This difference in behaviour between the two modelling approaches reflects the self-regulating role of temperature-driven feedback processes related to dissipative structures.

In summary, the temporal evolution of the elasto-visco-plastic models suggests that energy dissipation, expressed by an evolving network of shear zones, is regulated by minimization of stored energy, which leads to very similar values of the global stored energy (Figs. 3a and 4a), independent of applied velocity (Fig. 5a). These results contrast with expectations based on visco-plastic models, lacking thermal feedback processes, for which model strengths behave similarly to predictions from Brace–Goetze strength profiles. Most significantly, despite the complexity of local deformation, the integrated behaviour of the lithosphere becomes essentially that of an elasto-plastic solid with a single value of yield strength. For plate tectonic conditions this value is insensitive to strain rate, rheological stratification, or thermal structure. Feedback effects that allow for internal regulation of energy dissipation are the cause for convergence of elastic strengths. In contrast, we find that the ability of the lithosphere to resist a given applied force is significantly dependent on changes in its elastic properties.

4.2. Effect and nature of dissipation

The time integrated energy dissipation or shear heating for one model is shown in Fig. 7. Dissipation in the upper mantle produced heat capable of raising temperatures by ~ 100 K. Because some of this heat has diffused, the actual impact on local temperature is not as large. Given the volume of the high dissipation region (grey, red and orange in Fig. 7), this heat is a significant additional heat source to the radiogenic and the mantle heat flow, that must be considered in models of thermal evolution of deforming lithospheres. Its impact in the evolution of lithospheric deformation is marked by the gradual decrease in stored energy (Fig. 4). Fig. 7 shows that high energy dissipation, does not coincide with narrow shear bands, but covers a broad region of the upper mantle. This is because shear zones in the models are stable only at time scales of ~ 1 Myr, during which they reach a width of 5–10 km and heat up internally by ~ 10 K. Since strain weakening effects are operating at the time-scale of 0.1–1 Myr, the thermal diffusion of heat implies very wide shear zone migration.

5. Discussion

The similarity in stored energies for all models in Fig. 4a is attributed to self-organization of dissipative structures (Prigogine, 1978). In our models, these dissipative structures are manifested as wide and narrow shear bands. Widespread, penetrative deformation is less efficient in weakening the system than localized deformation. Thus, increased heat flow has two counteracting effects: it thermally weakens the lithosphere as a whole, but makes shear heating less efficient. Similarly, for a given heat flow, a thicker crust implies a hotter Moho temperature and weaker lithosphere due to the absence of a cold olivine-dominated shallow mantle, but this inhibits strain localization in the mantle reducing the efficiency of shear heating. The net effect is a similarity in the elastic strength for lithospheres with different heat flows and crustal thicknesses, as a result of a temperature self-regulation mechanism (Hartz and Podladchikov, 2008). This self-regulation results in a general convergence of the elastic strength evolution in time (Fig. 4a).

The thermodynamic principles in the calculations explain this self-regulation. The numerical solutions follow the principle of maximum dissipation (Martyushev and Seleznev, 2006), which is a stronger form of the second law of thermodynamics. Strain localization takes place along the maximum shear stress trajectories, implying maximum shear heating. In order to ensure maximum global dissipation, the system self-organizes, out of all possibilities, into a geometry that maximizes heat generation. Self-organization leads to the convergence of time-dependent elastic strength towards a low common value (Figs. 3 and 4a), as well as to the richness of dissipative structures (Fig. 2).

Self-organization here is a time-dependent process. In the models, shear bands are the main dissipative structures, and self-regulation controls their number and width, and consequently their strain rates and heat generation, as well as their temporal evolution. Localization phenomena controlling self-regulation are thought to require a threshold value for energy input into the system (Braeck and Podladchikov, 2007; Regenauer-Lieb and Yuen, 2004). However, Fig. 5a shows a similar strength evolution in calculations with an order of magnitude lower boundary velocity than the one used in Fig. 4. We conclude therefore that the threshold for self-regulation is below typical boundary velocities in deforming plates. For velocities above the threshold, but still within the range of plate tectonics, elastic lithospheric strength is independent of velocity.

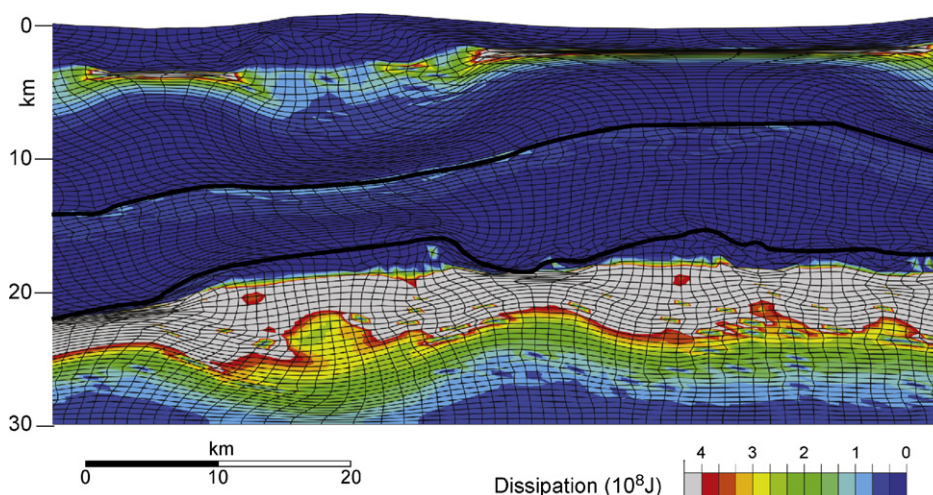


Fig. 7. Plot of time integrated dissipated energy for model in Fig. 2a at the same final time step (13.7 Ma, initial crustal thickness of 50 km, and heat flux of 50 mW/m²). Regions in grey below the Moho produce more than 4×10^8 J of heat, equivalent to a temperature increase, if not diffused, of more than 100 K. Temperature can be calculated from the diagram by dividing the dissipation by ρC_p (e.g. $\rho = 3000$ kg/m³, $C_p = 1000$ J/kg K).

The common curve recognized in all models in Fig. 4a can be seen also as resulting from the minimization of stored energy for the given elastic properties of the model lithosphere. This process is akin to recrystallization at grain scale, through which crystals minimize stored energy by removing high energy dislocations. It follows that the results are not particularly sensitive to changes in plastic and viscous properties of the lithosphere within the range of values used here. This is demonstrated by the fact that changes in initial Moho depth in the models, which effectively modify the global rheology of the models, do not significantly affect the evolution of the elastic strength (Fig. 4a).

The fundamental control on lithospheric strength is instead a combination of both the elastic properties of the lithosphere (Fig. 5b) and the strain accumulated during a single stress loading/deformation event (here expressed as the β factor, Figs. 4 and 5). The elastic properties control the energy that the system is capable of storing, and therefore regulate the ratio between stored and dissipated energy. Higher values of elastic properties (stiffer systems) would weaken the lithosphere because more energy would be dissipated into heat. This shifts the position of the strength curves (compare Figs. 4 and 5). The accumulated strain history (β factor) during a single deformation event controls where in the strength evolution curve a particular lithosphere is (e.g., Fig. 4a). The system is thus time-dependent and the lithosphere weakens as straining progresses. As expected from natural systems controlled by entropy, this implies that deformation history is a key factor controlling lithospheric strength and that at a given time, two lithospheres with similar elastic properties deforming at different velocities will have different strengths because of their different positions in the strength evolution curve.

The results can be expressed schematically in a stress–strain curve akin to that in Fig. 1, where different lithospheres were expected to yield at different stresses due to their different integrated visco-plastic behaviour. Instead, energy storage minimization combined with the ability of the system to self-regulate through feedback processes, have led to the development of similar curves defining a single value of yield strength (Fig. 8) for the given elastic properties of the models.

In summary, lithospheric deformation in our elasto-viscoplastic models start with an effectively elastic response characterized by a linear relationship between stress and strain. In this stage each of the three rheological layers in the model (quartz, feldspar, olivine) develop a strong elastic core region that stores most of the energy, and dissipation is restricted to shallow crust deforming plastically, or hot zones in each layer, deforming viscously. With time, less energy is stored while the elastic cores are gradually thinned as more energy is dissipated (Fig. 4). The overall effect is a degradation of the elastic strength with increasing β

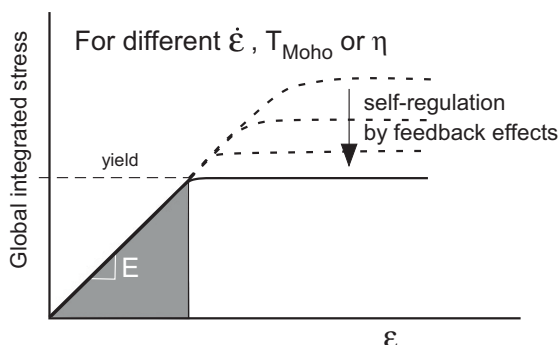


Fig. 8. Schematic stress–strain curves showing the effect of energy feedback processes on lithospheric strength. For models with the same elastic modulus (E) but different strain rate, Moho temperature or viscosity, the curves collapse to a single curve, controlled by the elastic modulus and yield strength.

factor. Models with the same elastic properties all yield at a similar time, (i.e., similar total strain) (Fig. 4). This point is marked by a similar value of stored energy (within 25% of each other) but variable energy dissipation: the coldest and thinnest models requiring more energy dissipation to weaken sufficiently so as to store the same amount of energy. Following this point, the elastic cores were broken up by dissipative structures and any energy added to the system is dissipated. The stored energy at yield (a measure of the unit force necessary to deform the boundary at a fixed velocity and a definition of strength) is independent of lithospheric geothermal structure, rheological stratification and boundary velocity, but dependent only on elastic properties (Fig. 5b). This convergence of strength results from the ability of the system to organize energy dissipation in order to minimize stored energy. In this way, large variations in expected lithospheric strength, collapsed to a single value, independent of flow laws, thermal structure and boundary velocity (Fig. 8).

6. Conclusions

In this paper we defined a useful measure of solid mechanical strength that includes information about the elastic properties and the yield stress of the lithosphere. This definition is necessary for understanding and modelling how energy is stored and dissipated when the lithosphere is deformed. We found that through thermal self-regulation and self-organization of dissipative structures (shear zones), different lithospheres that have the same elastic properties, define similar elastic strength evolution curves independent of bulk strain rate. This time-dependent process contrasts with the currently prevalent perception that strength is fundamentally controlled by the average strain rate, the initial steady-state temperature distribution (Molnar, 1992; O'Neill et al., 2008; Sandiford and McLaren, 2002), and the chemical and rheological composition of the lithosphere (Jackson et al., 2008; Lee et al., 2001). Thus, contrary to the perception that lithospheric strength is controlled primarily by thermal structure and its fluid response, we suggest that, in a global sense, strength depends on the ability of the lithosphere to store energy, which regulates self-organizing dissipative structures so as to yield at the same yield point. The integrated response of the lithosphere is thus that of an elasto-plastic solid with a fixed value of yield strength for given elastic properties. We conclude that more attention should be given to the choice and evolution of elastic properties in the assessment of continental strength. Elastic strength can be, for instance, significantly affected by damage of the lithosphere, in particular for large strains. Recent results (Karrech et al., 2011a,b,c) show that an order of magnitude in reduction of strength (Fig. 5b) can be locally introduced by damage, thereby potentially explaining the longevity of plate tectonic boundaries.

Acknowledgments

This manuscript has benefited from discussion and comments by Ali Karrech, Kenni Dinesen Petersen and Vladimir Lyakhovskiy. Research was funded by ARC Discovery Project DP1094050. KRL acknowledges support through the iVEC Supercomputer program, the Western Australian Premiers Fellowship and the Western Australian Geothermal Centre of Excellence.

References

- ABAQUS/Standard, 2000. User's Manual vol. 1, Version 6.1. Hibbit, Karlsson and Sorenson Inc., Pawtucket, Rhode Island.
- Afonso, J.C., Ranalli, G., 2004. Crustal and mantle strengths in continental lithosphere: is the jelly sandwich model obsolete? *Tectonophysics* 394, 221–232.
- Braeck, S., Podladchikov, Y.Y., 2007. Spontaneous thermal runaway as ultimate failure mechanism of materials. *Phys. Rev. Lett.* 98, 095504.

- Buck, W.R., 2006. The role of magma in the development of the Afro-Arabian Rift System. In: Yirgu, G., Ebinger, C.J., Maguire, P.K.H. (Eds.), *The Afar Volcanic Province within the East African Rift System*. Geological Society, Special Publications, London, pp. 43–54.
- Burov, E., Jaupart, C., Mareschal, J.C., 1998. Large-scale crustal heterogeneities and lithospheric strength in cratons. *Earth Planet. Sci. Lett.* 164, 205–219.
- Burov, E.B., 2010. The equivalent elastic thickness (T_e), seismicity and the long-term rheology of continental lithosphere: Time to burn-out “crème brûlée”? Insights from large-scale geodynamic modeling. *Tectonophysics* 484, 4–26.
- Burov, E.B., Watts, A.B., 2006. The long-term strength of continental lithosphere: “Jelly sandwich” or “crème brûlée”? *GSA Today* 16, 4–10.
- Chrysochoos, A., Belmahjoub, F., 1992. Thermographic analysis of thermomechanical couplings. *Arch. Mech.* 44, 55–68.
- Goetze, C., Evans, B., 1979. Stress and temperature in the bending lithosphere as constrained by experimental rock mechanics. *Geophys. J. R. Astr. Soc.* 59, 463–478.
- Hartz, E.H., Podladchikov, Y.Y., 2008. Toasting the jelly sandwich: the effect of shear heating on lithospheric geotherms and strength. *Geology* 36, 331–334.
- Hirth, G., Kohlstedt, D., 2004. Rheology of the upper mantle and the mantle wedge: a view from the experimentalists. In: Eiler, J. (Ed.), *The Subduction Factory*, American Geophysical Union, Washington, pp. 83–105.
- Jackson, J., 2002. Strength of the continental lithosphere; time to abandon the jelly sandwich? *GSA Today* 12, 4–10.
- Jackson, J., McKenzie, D., Priestley, K., Emmerson, B., 2008. New views on the structure and rheology of the lithosphere. *J. Geol. Soc.* 165, 453–465.
- Karrech, A., Regenauer-Lieb, K., Poulet, T., 2011a. Continuum damage mechanics for the lithosphere. *J. Geophys. Res.* 116, art. no. B04205.
- Karrech, A., Regenauer-Lieb, K., Poulet, T., 2011b. Frame indifferent elastoplasticity of frictional materials at finite strain. *Int. J. Solids Struct.* 48, 407.
- Karrech, A., Regenauer-Lieb, K., Poulet, T., 2011c. A damaged visco-plasticity model for pressure and temperature sensitive geomaterials. *Int. J. Eng. Sci.* 49, 1141–1150.
- Kaus, B.J.P., Podladchikov, Y.Y., 2006. Initiation of localized shear zones in viscoelastoplastic rocks. *J. Geophys. Res.* 111, B04412, doi:04410.01029/02005JB003652.
- Kirby, S.H., Kronenberg, A.K., 1987a. Correction to “Rheology of the lithosphere: Selected topics” by S. H. Kirby and A. K. Kronenberg. *Rev. Geophys.* 25, 1680–1681.
- Kirby, S.H., Kronenberg, A.K., 1987b. Rheology of the lithosphere: selected topics. *Rev. Geophys.* 25, 1219–1244.
- Kohlstedt, D.L., Evans, B., Mackwell, S.J., 1995. Strength of the lithosphere: constraints imposed by laboratory experiments. *J. Geophys. Res.* 100, 17,587–517,602.
- Kusznir, N.J., 1982. Lithosphere response to externally and internally derived stresses: a viscoelastic stress guide with amplification. *Geophys. J. R. Astr. Soc.* 70, 399–414.
- Kusznir, N.J., Park, R.G., 1982. Intraplate lithosphere strength and heat flow. *Nature* 299, 540–542.
- Kusznir, N.J., Park, R.G., 1984. Intraplate lithosphere deformation and the strength of the lithosphere. *Geophys. J. R. Astr. Soc.* 79, 513–538.
- Lee, C.T., Yin, Q., Rudnick, R.L., Jacobsen, S.B., 2001. Preservation of ancient and fertile lithospheric mantle beneath the southwestern United States. *Nature* 411, 69–73.
- Maggi, A., Jackson, J.A., McKenzie, D., Priestley, K., 2000. Earthquake focal depths, effective elastic thickness, and the strength of the continental lithosphere. *Geology* 28, 495–498.
- Martyushev, L.M., Seleznev, V.D., 2006. Maximum entropy production principle in physics, chemistry and biology. *Phys. Rep.* 426, 1–45.
- Molnar, P., 1992. Brace–Goetze strength profiles, the partitioning of strike-slip and thrust faulting at zones of oblique convergence, and the stress-heat flow paradox of the San Andreas Fault. In: Evans, B., Wong, T.F. (Eds.), *Fault Mechanics and Transport Properties of Rocks; A Festschrift in Honor of W. F. Brace*. Acad. Press, San Diego, pp. 435–459.
- Moresi, L., Solomatov, V., 1998. Mantle convection with a brittle lithosphere: thoughts on the global tectonic styles of the Earth and Venus. *Geophys. J. Int.* 133, 669–682.
- O'Neill, C.J., Lenardic, A., Griffin, W.L., O'Reilly, S.Y., 2008. Dynamics of cratons in an evolving mantle. *Lithos* 102, 12–24.
- Pérez-Gussinyé, M., Morgan, J.P., Reston, T.J., Ranero, C.R., 2006. The rift to drift transition at non-volcanic margins: insights from numerical modelling. *Earth Planet. Sci. Lett.* 244, 458–473.
- Perry, H.K.C., Mareschal, J.C., Jaupart, C., 2006. Variations of strength and localized deformation in cratons: the 1.9 Ga Kapuskasing uplift, Superior Province, Canada. *Earth Planet. Sci. Lett.* 249, 216–228.
- Poulet, T., Regenauer-Lieb, K., Karrech, A., 2010. A unified multi-scale thermodynamic framework for coupling geomechanical and chemical simulations. *Tectonophysics* 483, 178–189.
- Prigogine, I., 1978. Time, structure, and fluctuations. *Science* 201, 777–785.
- Ranalli, G., Murphy, D.C., 1987. Rheological stratification of the lithosphere. *Tectonophysics* 132, 281–295.
- Regenauer-Lieb, K., Karrech, A., Chua, H.T., Horowitz, F.G., Yuen, D., 2010. Time-dependent, irreversible entropy production and geodynamics. *Phil. Trans. R. Soc.* 368, 285–300.
- Regenauer-Lieb, K., Rosenbaum, G., Weinberg, R.F., 2008. Strain localisation and weakening of the lithosphere during extension. *Tectonophysics* 458, 96–104.
- Regenauer-Lieb, K., Weinberg, R.F., Rosenbaum, G., 2006. The effect of energy feedbacks on continental strength. *Nature* 442, 67–70.
- Regenauer-Lieb, K., Yuen, D.A., 2003. Modeling shear zones in geological and planetary sciences: solid- and fluid-thermal-mechanical approaches. *Earth-Sci. Rev.* 63, 295–349.
- Regenauer-Lieb, K., Yuen, D.A., 2004. Positive feedback of interacting ductile faults from coupling of equation of state, rheology and thermal-mechanics. *Phys. Earth Planet. Int.* 142, 113–135.
- Regenauer-Lieb, K., Yuen, D.A., Fusses, F., 2009. Landslides, ice quakes, earthquakes: a thermodynamic approach to surface instabilities. *Pure Appl. Geophys.* 166, 1885–1908.
- Rosenbaum, G., Regenauer-Lieb, K., Weinberg, R.F., 2010. Interaction between mantle and crustal detachments: a non-linear system controlling basin formation. *J. Geophys. Res.* 115, B11412, doi:10.1029/2009JB006696.
- Sandiford, M., McLaren, S., 2002. Tectonic feedback and the ordering of heat producing elements within the continental lithosphere. *Earth Planet. Sci. Lett.* 204, 133–150.
- Schmalholz, S.M., Kaus, B.J.P., Burg, J.P., 2009. Stress–strength relationship in the lithosphere during continental collision. *Geology* 37, 775–778.